Photosynthetic Electron Transfer from Reaction Center Pigment−Protein Complex in Silica Nanopores

ARTICLE *in* LANGMUIR · AUGUST 2010

Impact Factor: 4.46 · DOI: 10.1021/la101810v · Source: PubMed

10 AUTHORS, INCLUDING:

Mamoru Nango
Osaka City University
243 PUBLICATIONS **2,559** CITATIONS

SEE PROFILE

Shigeru Itoh
Nagoya University
222 PUBLICATIONS **4,125** CITATIONS

SEE PROFILE

Langmuir
Article
pubs.acs.org/Langmuir

Photosynthetic Electron Transfer from Reaction Center Pigment−Protein Complex in Silica Nanopores

Ippei Oda,[†] Masayo Iwaki,[‡,∥] Daiju Fujita,[†] Yasutaka Tsutsui,[†] Souji Ishizaka,[†] Makiko Dewa,[§] Mamoru Nango,[§] Tsutomu Kajino,[⊥] Yoshiaki Fukushima,[⊥] and Shigeru Itoh*[,†]

[†]*Division of Material Science Physics, Graduate School of Science, Nagoya University, Furo-cho, Chikusa-ku Nagoya, Aichi 464-8602, Japan,* [‡]*Glynn Laboratory of Bioenergetics, Department of Biology, University College London, Gower Street, London WC1E 6BT, U.K.,* [§]*Department of Applied Chemistry, Graduate School of Engineering, Nagoya Institute of Technology, Gokiso-cho, Nagoya 466-8555, Japan, and* [⊥]*Toyota Central R&D Laboratories, Inc., Yokomichi, Nagakute, Aichi 480-1192, Japan.* [∥]*Present address: Toyota Central R&D Laboratories, Inc. Yokomichi, Nagakute, Aichi 480-1192, Japan.*

Received May 6, 2010. Revised Manuscript Received June 23, 2010

A photosynthetic reaction center (RC) pigment−protein complex purified from a thermophilic purple photosynthetic bacterium, *Thermochromatium tepidum*, was adsorbed to a folded-sheet silica mesoporous material (FSM). The RC has a molecular structure with a 7.0 × 5.0 × 13 nm diameter. The amount of RC adsorbed to the FSM compound with an average internal pore diameter of 7.9 nm ($FSM_{7.9}$) was high at 0.29 gRC/gFSM, while that to the $FSM_{2.7}$ (2.7 nm diameter) was low at 0.02 gRC/gFSM, suggesting the specific binding of the RC into the 7.9 nm pores of $FSM_{7.9}$. An N_2-adsorption isotherm study indicated the incorporation of the RC into the 7.9 nm pores. The RC inside $FSM_{7.9}$ showed absorption spectra in the visible and infrared regions similar to those of the RC in solution, indicating almost no structural changes induced by the adsorption. The RC−$FSM_{7.9}$ conjugate showed the high photochemical activity with the increased thermal stability up to 50 °C in the measurements by laser spectroscopy. The conjugates rapidly provided electrons to a dye in the outer medium or showed electric current on the ITO electrode upon the illumination. The RC−FSM conjugate will be useful for the construction of artificial photosynthetic systems and new photodevices.

Introduction

Mesoscopic silica materials have been used as the adsorbents for organic and biological materials to develop new types of functional materials.[1−4] Various silica materials, which have inner pores with diameters of nanometer sizes, have been produced and used to adsorb functional organic compounds or enzymes.[5−15] FSM (folded-sheet mesoporous material),[4] SBA,[12] and MPS,[11] which are made of silica with ordered hexagonal pores of several nanometer diameters, have been produced. The materials adsorb functional organic molecules such as chlorophyll *a*[5−7] or soluble proteins such as horseradish peroxidase (with a molecular mass of 44 kDa),[9,10] cytochrome *c* (12.3 kDa),[11,12] lysozyme (14.4 kDa),[13] or catalase (440 kDa).[3] The absorptions preserved their activities and sometimes increased the stabilities of the incorporated molecules.[1−8]

Biomembranes contain various functional protein complexes that bear important biological functions, such as energy conversion, sensory responses, metabolite transports, and detoxification. However, these complexes are usually water-insoluble and can be functional only in liposomes or detergent micelles after their extraction and purification with detergents. The utilization of these activities in artificial environments has been awaited. Photosynthetic systems, which convert solar energy to chemical energy to synthesize organic materials, also reside on the inner membranes of plant chloroplasts and bacterial cells. The activity has been supplying most of the energy for life on earth and provided molecular oxygen into the atmosphere. We, however, have not yet successfully constructed an artificial photosynthetic system with comparable high efficiency. Here, we report an attempt to realize biological photosynthesis inside nanopores in fabricated silica mesoscopic material FSM.

We reported the adsorption of the light-harvesting-2 pigment−protein complex (LH2) isolated from a thermophilic purple photosynthetic bacterium, *Thermochromatium* (*Tch.*) *tepidum*, with a molecular mass of 129 kDa, into FSM nanopores.[15] LH2 adsorbed to the FSM retained the native function to harvest light energy with increased heat stability of the structure. In this study, we introduced a photosynthetic reaction center (RC) pigment−protein complex purified from *Tch. tepidum* into silica nanopores and tested its function. *Tch. Tepidum* grows at the highest temperature among all the purple photosynthetic bacteria, with a

*To whom correspondence should be addressed: Ph +81(52) 789 4739; Fax +81(52) 789 4739; e-mail itoh@bio.phys.nagoya-u.ac.jp.

(1) Knopp, D.; Dianping, T.; Niessner, R. *Anal. Chim. Acta* **2009**, *647*, 14–30.
(2) Humphrey, H.; Yiua, P.; Wright, P. A. *J. Mater. Chem.* **2005**, *15*, 3690–3700.
(3) Wang, Y.; Caruso, F. *Chem. Mater.* **2005**, *17*, 953–961.
(4) Fukushima, Y.; Inagaki, S. *Mater. Sci. Eng., A* **1996**, *217/218*, 116–118.
(5) Itoh, T.; Yano, K.; Inada, Y.; Fukushima, Y. *J. Am. Chem. Soc.* **2002**, *124*, 13437–13441.
(6) Itoh, T.; Yano, K.; Inada, Y.; Fukushima., Y. *J. Mater. Chem.* **2002**, *12*, 3275–3277.
(7) Itoh, T.; Yano, K.; Inada, Y.; Kajino, T.; Itoh, S.; Shibata, Y.; Mino, H.; Miyamoto, R.; Inada, Y.; Iwai, S.; Fukushima, Y. *J. Phys. Chem. B* **2004**, *108*, 13683–13687.
(8) Takahashi, H.; Li, B.; Sasaki, T.; Miyazaki, C.; Kajino, T.; Inagaki, S. *Microporous Mesoporous Mater.* **2001**, *44*−*45*, 755–762.
(9) Deere, J.; Magner, E.; Wall, J. G.; Hodnett, B. K. *Catal. Lett.* **2003**, *85*, 19–23.
(10) Deere, J.; Magner, E.; Wall, J. G.; Hodnett, B. K. *Chem. Commun.* **2001**, *5*, 465–466.
(11) Vinu, A.; Murugesan, V.; Tangermann, O.; Hartmann, M. *Chem. Mater.* **2004**, *16*, 3056–3065.
(12) Fan, J.; Lei, J.; Wang, L.; Yu, C.; Tu, B.; Zhao, D. *Chem. Commun.* **2003**, *17*, 2140–2141.
(13) Pandya, P. H.; Jasra, R. V.; Newalkar, B. L.; Bhatt, P. N. *Microporous Mesoporous Mater.* **2005**, *77*, 67–77.
(14) Kato, K.; Irimescu, R.; Saito, T.; Yokogawa, Y.; Takahashi, H. *Biosci. Biotechnol. Biochem.* **2003**, *67*, 203–206.
(15) Oda, I.; Hirata, K.; Watanabe, S.; Shibata, Y.; Kajino, T.; Fukushima, Y.; Iwai, S.; Itoh, S. *J. Phys. Chem. B* **2006**, *110*, 1114–1120.

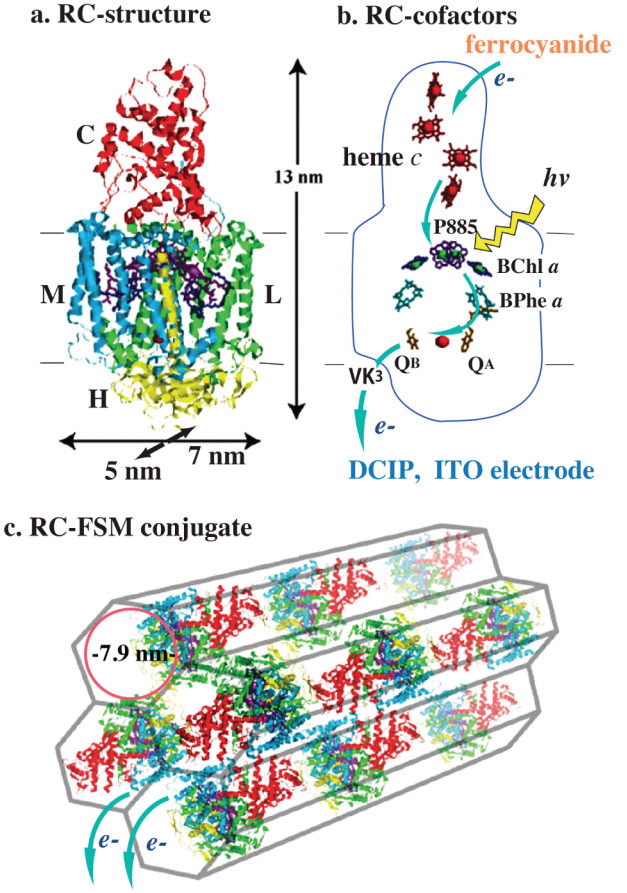

Figure 1. Structure of the RC complex (a), electron transfer cofactors and pathway inside the RC (b), and a schematic view of the RC inside silica nanopores in $FSM_{7.9}$ (c). L, M, H, and C in (a) represent names of subunit polypeptides.

maximum growth temperature at 58 °C.[16,17] The RC complex of *Tch. tepidum* is stable up to 70 °C in native membranes and to 35−48 °C in detergent micelles after isolation.[18] The RC complex contains four polypeptide subunits, L, M, H, and C[18−24] (as shown in Figure 1) that bind the redox cofactors for photosynthetic charge separation and electron transfer reactions, including the primary electron donor P885, which is a special pair of bacteriochlorophyll *a* (BChl *a*).[18,20,24] Light-excited P885 donates an electron to the electron acceptor bacteriopheophytin *a* (BPhe) within a few picoseconds and to the electron acceptor menaquinone Q_A in less than 1 ns. $P885^+$, then, is rereduced by an electron from one of four hemes *c* in the C subunit. Inside the intact membranes, most parts of the L and M subunits seen in Figure 1 are surrounded by hydrophobic hydrocarbon tails of fatty acid of lipids so that these moieties should be covered by some hydrophobic materials, such as hydrocarbon tails of detergents after the extraction. A recent study demonostrated the incorporation of the His-tagged RC complex (with a gold nanoparticle) isolated from a photosynthetic purple bacterium, *Rhodobacter*(*Rb.*) *sphaeroides*, into carbon nanotubes that are rather hydrophobic and electrically conductive, with detergent molecules.[25] The RCs showed output of photoelectrical currents. Here, we report the function and structure of RC in electrically nonconductive silica nanopores.

We introduced the thermally stable RC complex of *Tch. tepidum* into the silica nanopores inside the FSM and measured the light-induced output of electrons from the RC to the electrode or to a redox dye in the outer medium. The adsorption to the FSM stabilized the RC structure and enabled its function at the higher temperature. The arrangement and packing of RC inside silica nanopores estimated based on the results in this study are schematically shown in Figure 1C.

Materials and Methods

Tch. tepidum cells were grown anaerobically at 50 °C as reported.[14,15] The RC protein was extracted from the membranes of *Tch. tepidum* by the treatment with a detergent, lauryldimethylamine oxide (LDAO), at 0.25% at 40 °C for 30 min and purified by anion-exchange chromatography as reported.[26,27] The molecular weight of the RC with C subunit was 137 kDa. The molar extinction coefficient at 800 nm (ε_{800}) of the RC was estimated to be 288 mM^{-1} cm^{-1}, similar to that determined in the RC of *Rb. sphaeroides*.[28]

FSM with an estimated average pore diameter of 2.7, 7.9, or 9.0 nm (designated $FSM_{2.7}$, $FSM_{7.9}$, or $FSM_{9.0}$, respectively, in this study) was prepared from kanemite (layered polysilicate). $FSM_{2.7}$ was prepared from kanemite using hexadecyltrimethylammonium chloride as described by Inagaki et al.,[29] who first reported the formation of FSM with a honeycomb hexagonal structure. $FSM_{7.9}$ and $FSM_{9.0}$ were prepared by essentially the same method[29] as that for $FSM_{2.7}$ using hexadecyltrimethylammonium chloride and 1,3,5-triisopropylbenzene (TIPB) in the molar ratio of TIPB/surfactant = 3.4 and docosyltrimethylammonium chloride and TIPB in the molar ratio of TIPB/surfactant = 4, respectively. The average pore diameters of the FSM materials were calculated from the N_2 adsorption isotherm curves (like those in Figure 3) according to the BJH method.[30]

Adsorption of the RC to the FSM was performed as reported for LH2[15] as follows: 1 mg of dry powder of FSM was added to a 1 mL solution of 0.01−0.5 mg/mL RC protein containing a 20 mM Tris-HCl buffer (pH 8.5), 0.03% LDAO, and 300 mM NaCl. The mixture was gently stirred at 30 °C for 2 h to saturate adsorption. The amount of adsorbed RC protein was spectrophotometrically estimated by measuring the absorbance decrease in the supernatant at 800 nm with a double-beam double-monochromator spectrophotometer (UV-3100PC, Shimadzu, Kyoto, Japan) after centrifugation to sediment the RC−FSM conjugate. The amount was also determined by the direct measurement of absorption spectrum of suspension of RC−FSM conjugate by the fiber spectroscope (see Figure 2A).

The adsorption of RC inside the pores of the FSM was also tested by the measurement of N_2 adsorption isotherms at 77 K using a Quantachrome AS-1 (Quantachrome, Boynton Beach, FL). The pore diameter distribution curves were derived from the N_2 adsorption isotherm curves by the BJH method.[30] We

(16) Madigan, M. T. *Science* **1984**, *225*, 313–315.
(17) Madigan, M. T. *Int. J. Syst. Bacteriol.* **1986**, *36*, 222–227.
(18) Nozawa, T.; Fukada, T.; Hatano, M.; Madigan, M. T. *Biochim. Biophys. Acta* **1986**, *852*, 191–197.
(19) Garcia, D.; Parot, P.; Verméglio, A. *Biochim. Biophys. Acta* **1987**, *894*, 379–385.
(20) Nozawa, T.; Trost, J. T.; Fukada, T.; Hatano, M.; McManus, J. D.; Blankenship, R. E. *Biochim. Biophys. Acta* **1987**, *894*, 468–476.
(21) Lancaster, C. R.; Michel, H. *Structure* **1997**, *5*, 1339–1359.
(22) Ivancich, A.; Kobayashi, M.; Drepper, F.; Fathir, I.; Saito, T.; Nozawa, T.; Mattioli, T. A. *Biochemistry* **1996**, *35*, 10529–10538.
(23) Nogi, T.; Fathir, I.; Kobayashi, M.; Nozawa, T.; Miki, K. *Proc. Natl. Acad. Sci. U.S.A.* **2000**, *97*, 13561–13566.
(24) Fathir, I.; Mori, T.; Nogi, T.; Kobayashi, M.; Miki, K.; Nozawa, T. *Eur. J. Biochem.* **2001**, *268*, 2652–2657.
(25) Lebedev, N.; Trammell, S. A.; Tsoi, S. *Langmuir* **2008**, *24*, 8871–8876.
(26) Kobayashi, M.; Nozawa, T. *Bull. Chem. Soc. Jpn.* **1993**, *66*, 3834–3836.
(27) Katayama, N.; Kobayashi, M.; Motojima, F.; Inaka, K.; Nozawa, T.; Miki, K. *FEBS Lett.* **1994**, *348*, 158–160.
(28) Straley, S. C.; Parson, W. W.; Mauzerall, D. C.; Clayton, R. K. *Biochim. Biophys. Acta* **1973**, *305*, 597–609.
(29) Inagaki, S.; Fukushima, Y.; Kuroda, K. *J. Chem. Soc., Chem. Commun.* **1993**, *8*, 680–682.
(30) Barrett, E. P.; Joyner, L. G.; Halenda, P. P. *J. Am. Chem. Soc.* **1951**, *73*, 373–380.

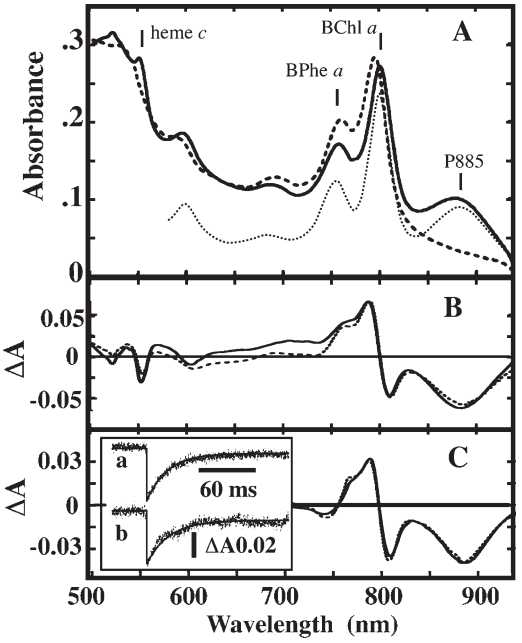

Figure 2. Absorption spectrum and redox reaction of RC adsorbed to $FSM_{7.9}$. (A) Absorption spectra of dithionite-reduced (solid line) and ferricyanide-oxidized (broken line) forms of the RC−$FSM_{7.9}$ conjugate. A dotted line represents the absorption spectrum of the dithionite-reduced RC in solution normalized to give the same RC concentration. (B) "Oxidized *minus* reduced" difference spectra of RC in solution (broken line) and of the RC−$FSM_{7.9}$ conjugate (solid line) calculated from the results in (A). (C) Flash-induced absorption changes of the RC in solution (broken line) and the RC−$FSM_{7.9}$ conjugate (solid line). The inset in (C) shows the time courses of the absorption change of P885 induced by the laser flash excitation (flash-induced oxidation and dark reduction): a, RC in solution; b, RC−$FSM_{7.9}$ conjugate. The RC and RC−$FSM_{7.9}$ conjugate were suspended in media containing 20 mM Tris-HCl buffer (pH 8.5) with and without 0.03% LDAO, respectively. No dithionite was added in (C) to keep the *c*-hemes to be oxidized to stop the rapid reduction of $P885^+$ after the flash excitations. The RC−$FSM_{7.9}$ suspensions were constantly stirred with a magnetic stirrer during the measurements.

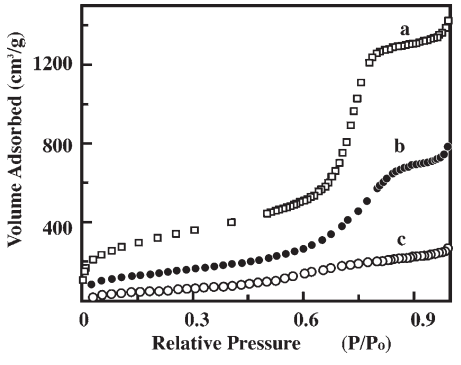

Figure 3. N_2 adsorption isotherm curves: (a) $FSM_{7.9}$ was treated with a medium containing 20 mM Tris-HCl at pH 8.5; (b) $FSM_{7.9}$ was treated with the same medium containing 0.03% (v/v) LDAO; (c) $FSM_{7.9}$ was treated with the same medium containing 0.03% (v/v) LDAO and RC at 0.22 g/g $FSM_{7.9}$. The ordinate indicates the adsorbed volume of N_2, and the abscissa indicates the ratio between the adsorption equilibrium pressure (P) and the saturated vapor pressure (P_0). See Materials and Methods for details.

prepared three samples: $FSM_{7.9}$, which was suspended in the reaction medium (1) with only a 20 mM Tris-HCl buffer (pH 8.5), (2) with LDAO, and (3) with RC at the same concentration of LDAO. The incubated FSM samples were then washed twice with a 20 mM Tris-HCl buffer (pH 8.5) and desiccated. The pore volume was estimated from the amount of adsorbed N_2 at the maximum relative pressure.

The absorption changes of the RC in a medium or in FSM were measured with a split beam spectrophotometer as described elsewhere.[18] The RC was chemically reduced by adding 0.1 mM sodium dithionite or oxidized by adding 0.1 mM potassium ferricyanide. The RC was also oxidized by illumination with a 532 nm flash light with 10 ns duration from a second harmonic of Nd:YAG laser (Quanta-Ray LAB-130-10TH, Spectra-Physics, Mountain View, CA).

The thermal stability of the photochemical activity of the RC was examined after heating samples at various temperatures for 10 min, and, then, the extent of the laser-induced absorption change of P885 at 885 nm was measured at 25 °C as described above.

A light-induced current was measured as described elsewhere[31] by adsorbing the RC or RC−$FSM_{7.9}$ conjugate to the surface of the indium tin oxide (ITO) electrode. The ITO electrodes were placed in a home-built reaction cell in a medium containing a 0.1 M phosphate buffer (pH 7.0), 0.1 M $NaClO_4$, and 5 mM methyl viologen. The reaction cell was made of three electrodes with a RC−$FSM_{7.9}$ adsorbed ITO electrode, a reference electrode (Ag/AgCl at a saturated KCl concentration), and a platinum flake counter electrode. Electric currents were induced by illumination of light at 890 nm to excite P885 specifically from a tungsten−iodine lamp through a monochromator and UV and heat-cut filters.

Fourier transform infrared (FTIR) spectra were measured with a Bruker IFS/66S FTIR spectrophotometer with a liquid nitrogen-cooled MCT-A detector at 4 ± 1 cm^{-1} resolution. An attenuated total reflection (ATR) unit with a 3-bounce 3 mm diameter Si prism and a ZnSe crystal (Smiths Detection) and a laboratory-made flow cell were set in the sample chamber.[32,33] Free detergent (LDAO) molecules contained in the RC stock solution were removed by repeated washings with distilled water before the measurements. For the measurement of the RC preparation, a 20 μL aliquot of the RC solution (at 0.1 mM in 20 mM Tris-HCl, pH 8.5) was diluted 100 times with distilled water, and then the RC complexes were precipitated by centrifugation (400000*g*, 1 h). The pellet was resuspended in water and precipitated again. The water wash was repeated twice, and the final pellet was suspended in 20 μL of distilled water. 2−3 μL of the water-washed RC suspension was deposited on the Si prism and dried with a gentle dry N_2 stream.

For the measurement of RC−$FSM_{7.9}$ conjugate, the RC−$FSM_{7.9}$ suspension (100 μL) was diluted 10 times with distilled water and precipitated by centrifugation (8000*g*, 2 min). The water wash was repeated three times, and the final pellet was suspended in 50 μL of water. A 2−3 μL aliquot of the suspension was deposited on the Si prism and dried. The dry layer was rehydrated with a buffer (10 mM potassium phosphate, 100 mM KCl, 2 mM $MgCl_2$, pH 7.5). For the measurement of $FSM_{7.9}$ alone, a 2−3 μL aliquot of $FSM_{7.9}$ suspended in distilled water (at 0.5 mg $FSM_{7.9}$/200 μL) was deposited on the Si prism and then dried.

The "dry" layers were rehydrated again with a detergent-free buffer and then subjected to the redox activity measurement by the perfusion-induced ATR-FTIR. Redox changes of P885 in the RC samples in the ATR flow cell were induced by switching between the perfusion buffers containing either 1.5 mM ferricyanide for oxidation or ferrocyanide for reduction as previously reported.[32] Extensive removal of the detergents from the starting material by the repeated wash and dry processes, which were

(31) Suemori, Y.; Nagata, M.; Nakamura, Y.; Nakagawa, K.; Okuda, A.; Inagaki, J.; Shinohara, K.; Ogawa, M.; Iida, K.; Dewa, T.; Yamashita, K.; Gardiner, A.; Cogdell, R. J.; Nango, M. *Photosynth. Res.* **2006**, *90*, 17–21.
(32) Iwaki, M.; Andrianambinintsoa, S.; Rich, P.; Breton, J. *Spectrochim. Acta, Part A* **2002**, *58*, 1523–1533.
(33) Rich, P. R.; Iwaki, M. *Mol. Biosyst.* **2007**, *3*, 398–407.

Table 1. Incorporation of Proteins into Silica Nanopores

protein name (molecular weight in kDa)	porous materials (average pore diameter in nm)	adsorbed amount (g/g silica)	conditions [reference], *this study
membrane proteins			
bacterial RC complex (137)	FSM (7.9)	0.29	with 0.003% LDAO*
	(2.7)	0.02	with 0.003% LDAO*
	(9.0)	0.10	with 0.003% Triton*
	(7.9)	0.08	with 0.003% Triton*
	(2.7)	0.02	with 0.003% Triton*
bacterial LH2 complex (129)	FSM (7.9)	1.11	[15]
soluble proteins			
horse radish peroxidase (44.0)	FSM (8.9)	0.18	[8]
cytochrome *c* (12.3)	MCM (2.8)	0.021	[10]
cytochrome *c* (12.3)	MPS-F127 (5.0)	0.084	[10]
lysozyme (14.4)	Rod-SBA (7.9)	0.53	[12]
hemoglobin (64.5)	HMS (6.5)		[12]
catalase (250)	BMS (2−40)	0.075	[3]

required to achieve good stability of the sample film attached to the ATR prism during flow, did not induce denaturation of the RC as reported.[32] Measurement of the "oxidized *minus* reduced" IR difference spectrum was done by recording 1000 interferograms (130 s) at the reduced state as a reference first and then at the oxidized state. The "reduced *minus* oxidized" spectrum was recorded by repeating the same procedure in the oxidative direction, too. The redox cycle was repeated 40 times, and the final spectra were obtained as an average of the "oxidized *minus* reduced" and the inverse of the "reduced *minus* oxidized" spectra. The sample was kept at 0−10 °C during the ATR sample preparation and at room temperature during the IR measurements.

Results

Adsorption of Purified Photosynthetic Reaction Center Complex to FSM. The photosynthetic RC pigment−protein complex purified from a thermophilic bacterium *Tch. tepidum* was adsorbed to the FSM by adding dry FSM powder into the RC solution under gentle stirring at 30 °C. The isolated RC is stable for more than 10 days at room temperature. The adsorption was easily detected by monitoring the increase of red color of RC onto the white FSM powder either directly or quantitatively as the decrease of RC absorbance in the supernatant after sedimentation of the RC−FSM conjugate. After incubation for 1 h, the adsorption of the RC to the FSM was almost saturated. The amounts adsorbed to $FSM_{2.7}$ and $FSM_{7.9}$, which have inner pore diameters of 2.7 and 7.9 nm, respectively, were determined to be 0.02 and 0.29 g/g FSM (Table 1). $FSM_{7.9}$, thus, binds 14.5 times larger amount of RC than $FSM_{2.7}$. The result showed that RC adsorption to FSM is very sensitive to the pore size. We also measured the amounts of FSM-adsorbed RC that was dissolved in the medium containing 0.03% Triton X-100 instead of 0.03% LDAO with $FSM_{2.7}$, $FSM_{7.9}$, and $FSM_{9.0}$ (Table 1). The adsorbed amounts were larger with FSM with larger pore diameters similarly to the case of RC dissolved with LDAO. We detected the adsorption of 0.08 g RC/g $FSM_{7.9}$ at 0.03% Triton X-100. The value was smaller than that of 0.29 g/g $FSM_{7.9}$ observed with the LDAO-dissolved RC, suggesting the stronger interaction of Triton X-100 with $FSM_{7.9}$. Indeed, when we added Triton X-100 into the suspension of the LDAO-dissolved RC−$FSM_{7.9}$ conjugate, we detected the partial release of the RC from the $FSM_{7.9}$ to the outer medium (not shown). Therefore, detergent molecules seem to bind to FSM in competition with the RC, and Triton X-100 has a stronger affinity to FSM than LDAO. We also detected the binding of LDAO to $FSM_{7.9}$ by N_2 adsorption isotherm measurements (see Figure 3).

$FSM_{2.7}$ and $FSM_{7.9}$ have similar physicochemical properties and particle sizes (2−5 μm)[4,29] except for the difference in the sizes of their inner pores. The diameters of the pores inside $FSM_{2.7}$ and $FSM_{7.9}$ are smaller and larger, respectively, than the molecular diameter of the RC, which has a cylindrical structure with a 5 × 7 nm cross section along the membrane surface and a 13 nm height along the membrane normal that is parallel to the longitudinal axis as shown in Figure 1. The side wall of the RC cylinder made of L and M subunits is hydrophobic and is embedded inside membrane lipids, and the top and bottom ends of the cylinder are hydrophilic to face the aqueous phases. The different amounts of adsorption to the FSM with different pore sizes (Table 1), together with the results obtained from the N_2 adsorption isotherm below, suggest that RC specifically binds to the nanopores inside $FSM_{7.9}$ and does not go into the smaller 2.7 nm nanopores in $FSM_{2.7}$. The bindings of RC to the outer surfaces of $FSM_{7.9}$ and $FSM_{2.7}$ would not be very different from each other because of their similarities in the particle sizes and physicochemical properties.

The absorption spectrum of the RC−$FSM_{7.9}$ conjugate (solid line in Figure 2A) suspended in the 20 mM Tris-HCl buffer (pH 8.5) under the reduced condition was very similar to that of the free RC measured in the aqueous medium (dotted line), except for the elevation of the baseline of the former due to the high light scattering from the FSM moiety, as shown in Figure 2.

N_2 Adsorption Isotherm Curves. Figure 3 shows the N_2 adsorption isotherm curves of $FSM_{7.9}$ treated with a 20 mM Tris-HCl buffer at pH 8.5 (curve a), with the same buffer solution containing 0.03% (v/v) LDAO (curve b), and with the buffer solution containing 0.03% (v/v) LDAO and RC at 0.22 g/g $FSM_{7.9}$ (curve c). The adsorbed volume of N_2 increased with the increase of the N_2 pressure. From curve a, we calculated the average pore diameter of the FSM to be 7.9 nm according to the BJH method.[30] The extent of adsorption of N_2 was decreased to 60% if $FSM_{7.9}$ was treated with the buffer containing 0.03% LDAO (curve b) and was almost zero after the adsorption of the RC (curve c), suggesting the full incorporation of the RC into the nanopores. It is also suggested that LDAO binds to FSM, but more weakly than to the RC. Therefore, we assume that the RC and detergent compete with each other in the binding to FSM. As shown in Table 1, another detergent, Triton X-100, seems to more strongly bind to FSM and to decrease the binding of the RC.

Function of the RC in the FSM. We added 0.1 mM sodium dithionite (solid line) and 0.1 mM potassium ferricyanide (broken line) to reduce and oxidize the special pair P885, respectively. The spectra were measured by a spectrophotometer equipped with optical fibers to minimize the effect of light scattering from the FSM powder. The spectrum in the reduced state showed absorption bands of the accessory BChl *a* at 800 nm, the special pair P885 at 880 nm, and the electron acceptor BPhe *a* at 758 nm as indicted

in the figure. The P885 band and the BPhe *a* band in Figure 2A show a 5 nm blue shift and a 3 nm red shift, respectively, from their counterparts in the RC in solution (dotted line).[18,20] Almost no spectral shift was detected in the BChl *a* band. The results indicate that the RC adsorbed to $FSM_{7.9}$ maintained almost native spectral features, although small shifts of the absorption peaks of P885 and BPhe *a* were detected. On addition of ferricyanide, the P885 peak disappeared, showing its full oxidation (Figure 2A, broken line). The oxidation also induced blue shifts of the absorption bands of BChl *a* at 800 nm and BPhe at 758 nm due to the electrostatic interaction with $P885^+$ as seen in the oxidized *minus* reduced difference spectrum in Figure 2B (solid line). The negative peaks at 550 and 525 nm in the difference spectrum correspond to bleaches of the α- and *β*-peaks of *c*-type hemes on the C subunit due to their oxidation, and the negative peak at 600 nm represents the bleaching of the Qx absorption band of P885. The difference spectrum of the RC−$FSM_{7.9}$ conjugate (solid line) was essentially the same as that of the RC in solution (broken line). It is, therefore, clear that all the RC complexes inside $FSM_{7.9}$ are fully reduced/oxidized by dithionite/ferricyanide added into the outer medium as the RC in solution. This indicates the rapid equilibration of electrons between the RC adsorbed on $FSM_{7.9}$ and the small molecular reagents in the outer medium. The movement of the RC complex itself inside $FSM_{7.9}$ might be limited, judging from the slow releasing rate of RC from $FSM_{7.9}$.

Photosynthetic Activities of the RC Inside $FSM_{7.9}$. We tested the photochemical activity of RC adsorbed to $FSM_{7.9}$. The inset to Figure 2C shows the time course of the laser flash-induced absorption change at 885 nm of P885 inside the RC-$FSM_{7.9}$ conjugate (at 0.29 g RC/g $FSM_{7.9}$) suspended in a 20 mM Tris-HCl buffer at pH 7.8 (b) and the RC dispersed in the same buffer solution with 0.03% LDAO (a). Solid lines represent the simulated curves. Flash excitation induced rapid bleach (oxidation) of the absorption band of P885 and a following slow dark recovery (the dark reduction of $P885^+$). The time constant of the major phase of dark reduction of $P885^+$ was 20 ms in both the RC-$FSM_{7.9}$ conjugate and the RC in solution. Figure 2C shows the laser-flash-induced difference spectra of the RC in solution (broken line) and in the RC-conjugated $FSM_{7.9}$ (solid line). The spectra, as well as the time courses, are almost the same in shapes and extents each other when normalized with the RC concentration, showing the fully active reaction of P885 in both cases. The difference spectra in Figure 2C are almost the same those in Figure 2B, showing that the flash excitation oxidized P885 in RC−$FSM_{7.9}$ properly as ferricyanide did. These results indicate that the light-induced charge separation and the subsequent electron transfer reactions inside the RC were almost unaffected even after the adsorption of the RC to $FSM_{7.9}$. The time course with slow dark reduction and the feature of difference spectrum suggest the light-induced electron transfer from P885 to BPhe and then to the electron acceptor menaquinone Q_A and the subsequent dark reduction of $P885^+$ via electrons through *c*-hemes. It is, therefore, concluded that the RC is fully photoactive inside FSM.

Structure of the RC Inside $FSM_{7.9}$ Studied by ATR-FTIR Measurements. The structural properties of the RC inside $FSM_{7.9}$ were also studied by ATR-FTIR. The sample was prepared as a thin dry layer on the Si ATR prism. The ATR-FTIR spectrum of a layer of the RC−$FSM_{7.9}$ conjugate is shown in Figure 4, trace a. The layer exhibited peptide amide I and II peaks at 1655 and 1540 cm^{-1}, respectively. The overall spectral features are essentially identical to those of the RC alone (Figure 4, trace b). A broad band at 1080 cm^{-1} in RC− $FSM_{7.9}$ was due to the Si−O stretch of FSM silica, as seen in $FSM_{7.9}$ without the RC (Figure 4, trace c).

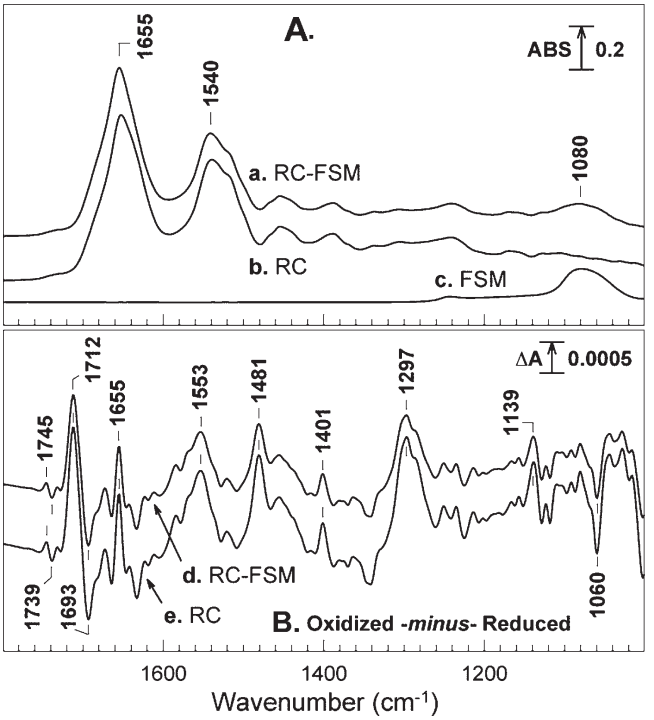

Figure 4. ATR-FTIR spectra of RC-$FSM_{7.9}$ conjugate. Upper panel: absolute ATR-FTIR spectra of the dry layer of RC-$FSM_{7.9}$ (a), free RC (b), and $FSM_{7.9}$ alone (c). Lower panel: perfusion-induced "oxidized *minus* reduced" difference ATR-FTIR spectra of RC-$FSM_{7.9}$ (d) and free RC (e). The redox changes were induced by switching two perfusion buffer solutions (0.1 M potassium phosphate, 0.1 M KCl, 2 mM $MgCl_2$, pH 7.5) containing 1.5 mM ferricyanide for oxidation and 1.5 mM ferrocyanide for reduction. Forty redox cycles of 1000 interferograms were averaged.

The perfusion-induced "oxidized *minus* reduced" ATR-FTIR spectra of RC−$FSM_{7.9}$ (trace d) and the free form of the RC (trace e) are shown in the lower panel of Figure 4. The oxidized or reduced form of the RC was generated reversibly by switching the perfusion buffer containing ferricyanide or ferrocyanide because the redox potential of the ferricyanide/ferrocyanide couple (E_m = + 430 mV SHE) is expected to be close to those of $P885^+$/P885 (E_m = +497 mV[22,34]) and high-potential cytochrome *c* hemes. The redox changes in P885 and hemes were confirmed by simultaneous optical measurements in the visible region (data not shown). RCs in $FSM_{7.9}$ and in a free form exhibited essentially identical spectral features with major bands at 1745(+), 1739(−), 1712(+), 1693(−), 1655(+), 1553(+), 1481(+), 1401(+), 1297(+), 1139(+), and 1060(−) cm^{-1} as well as minor bands.

Output of Electrons from the RC−$FSM_{7.9}$ Conjugate to Reagents Added into the Outer Medium. We tested the output of electrons from the RC in $FSM_{7.9}$. We added a dye, dichlorophenol indophenol (DCIP), into the reaction mixture and measured the flash-induced reduction of DCIP by the absorption decrease at 630 nm. In this experiment, we added potassium ferrocyanide as the electron donor to the heme *c* that gives electrons to the photo-oxidized P885 to prevent the charge recombination between $P885^+$ and reduced menasemiquinone$^-$ (Q_A^-) formed inside the RC (see Figure 1). DCIP cannot be reduced by ferrocyanide directly. DCIP and ferrocyanide mainly remained in the outer solution and were not specifically bound to $FSM_{7.9}$. A laser

(34) Noguchi, T.; Kusumoto, N.; Inoue, Y.; Sakurai, H. *Biochemistry* **1996**, *35*, 15428–15435.

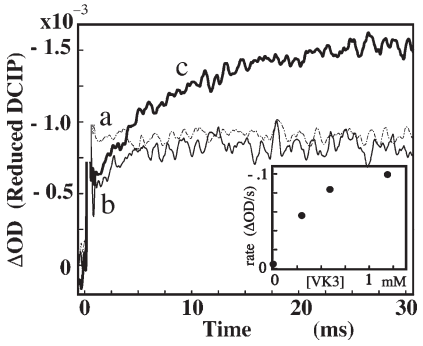

Figure 5. Laser-flash-induced reduction of dichloroindophenol (DCIP) dye by the RC−$FSM_{7.9}$ conjugate. Traces a, b, and c represent the laser-flash-induced absorption changes at 630 nm measured in the presence of 0, 0.25, and 1.2 mM vitamin K_3, respectively. The reaction mixture contained the RC−$FSM_{7.9}$ conjugate to give OD 0.1 at 800 nm, DCIP at 30 μM, and the reaction media as used in Figure 2. The inset figure shows the dependency of the rate of DCIP reduction (initial rate of the slow phase as shown in a−c traces) on the added concentration of vitamin K_3.

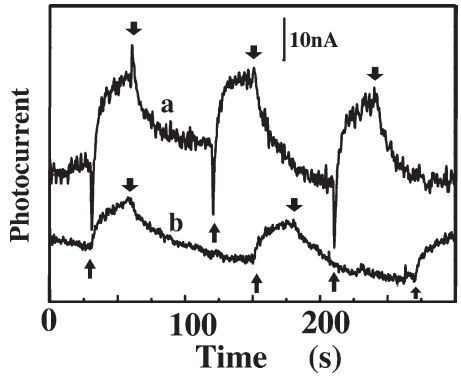

Figure 6. Photocurrents induced by the illumination of 890 nm continuous light of the RC (a) and the RC−$FSM_{7.9}$ conjugate (b) adsorbed to the surface of the ITO electrodes. Upward and downward arrows indicate the turn on and off of the illumination light, respectively. See Materials and Methods for the details of the experimental conditions.

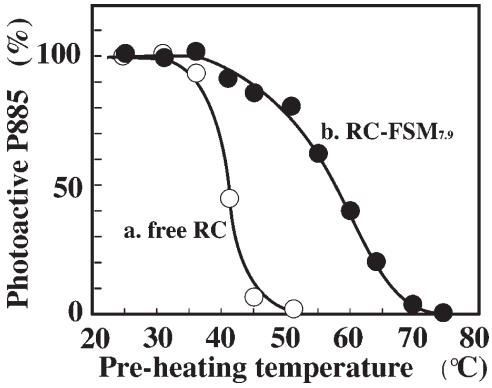

Figure 7. Effects of heat treatments on the photochemical activity of RC. Flash-light-induced absorption changes of P885 remaining after the heat treatment at the indicated temperatures were measured in the RC−$FSM_{7.9}$ conjugate (filled circles) and the free RC (open circles). Each sample was preheated at the indicated temperature for 10 min, and then the P885 photo-oxidation activities were measured at 25 °C.

flash excites P885 and reduces the electron acceptor menaquinone Q_A. The electron from Q_A^- is expected to reduce DCIP in the outer medium only when the electron transfer is mediated by the externally added menadione (vitamin K_3), as schematically shown in Figure 1. We detected no reduction of DCIP in the absence of VK_3 (a slow absorption decreasing phase in Figure 5, trace a) The very fast absorption decrease detected upon the flash excitation represents the bleach of Qy band of oxidized P885. Most of the flash-induced $P885^+$ was rapidly reduced by *c*-heme, and a small amount of $P885^+$ in the RC, which lacked reduced hemes, remained in the oxidized state at 1 ms (curve a). In the presence of 0.2 and 1.2 mM VK_3, different time courses with slow increasing phases of bleaching (reduction of DCIP) were detected (Figure 5, traces b and c). The initial rate of the DCIP reduction depended on the concentration of VK_3, as shown in the Figure 5 inset, which also includes the results of the measurements for the longer time scale. The final amount of reduced DCIP, which was determined by the competition between the reduction rate mediated by VK_3 and the oxidation rate by the air oxygen, was also increased. The initial rate of DCIP reduction became faster with the increase in the VK_3 concentration to 1.2 mM, indicating that the reduction of DCIP by the RC−$FSM_{7.9}$ conjugate is mediated by VK_3.

Electric Current on the ITO Electrode. We measured the light-induced photocurrent of the RC and the RC−$FSM_{7.9}$ conjugate that were adsorbed to the ITO electrode surface in the presence of a redox mediator, methyl viologen (Figure 6). The electric current was increased by the illumination at 890 nm and decreased in the dark after the illumination in the RC-adsorbed electrode. The RC−$FSM_{7.9}$ conjugate adsorbed to electrode also gave the photocurrent. The result, thus, indicates that the RC−$FSM_{7.9}$ conjugate gives photocurrent on the ITO electrode. A little different time courses and the lower photocurrent at the steady state of the RC−$FSM_{7.9}$ conjugate, even at the similar amounts of RC bound to the surface, might represent the situation that RC in the $FSM_{7.9}$ pore interacts with the electrode only indirectly beyond the silicate walls, probably mediated by dyes.

Increase in the Thermal Stability of the RC Structure/ Function Inside $FSM_{7.9}$. The thermal stability of the photochemical activity was examined for both the RC−$FSM_{7.9}$ conjugate and the RC in solution, as shown in Figure 7. Both samples were incubated at varied temperatures for 10 min, and then, the extent of the flash-oxidized P885 was measured at 25 °C, as shown in Figure 7 in each case. The activity did not change by the adsorption to FSM 7.9 by itself as already shown for Figure 2C; i.e., the 100% activities in both samples are almost the same in the absolute rates and extents. Figure 7 shows the amount of photochemically active P885 detected after the heat treatment. In the RC adsorbed to $FSM_{7.9}$, the amount of photo-oxidizable P885 did not decrease significantly until 60 °C (filled circles). On the other hand, the photochemical activity of RC in solution disappeared already after heating to 50 °C (open circles). It is also noted that the heat-induced inactivation of the RC−$FSM_{7.9}$ conjugate occurred in a temperature range (over a range of 40 °C at 35−75 °C) wider than that of the RC in solution (over a range of 20 °C at 30−50 °C), suggesting the higher heterogeneity inside $FSM_{7.9}$. After the heat denaturation, the RC also lost its characteristic absorption spectrum with the P885 peak showing the destruction of the structure. The result indicates that the adsorption to the silica nanopores protect the RC from heat damage, as reported for LH2 protein.[15] The adsorption to silica nanopores thus stabilizes the RC structure. This is interesting because the FTIR measurement in Figure 4 suggested almost no change of the RC protein structure at room temperature.

Discussion

Incorporation of the Reaction Center Protein into Silica Nanopores. The present study indicated that the photosynthetic RC protein that was incorporated into silica nanopores is fully active and performs the photosynthetic charge separation reaction and the electron transfer reactions if the pore diameter fits to the size of RC complex. An RC membrane protein of large molecular size (13 nm × 7 nm × 5 nm) that contains 4 large subunit proteins, 4 BChl *a*, 2 BPhe *a*, 2 menaquinone molecules, and 4 hemes *c* with a molecular mass of 137.0 kDa can be incorporated into silica nanopores that have inner pores with an average diameter size of 7.9 or 9.0 nm but not to one with a 2.7 nm diameter. Moreover, the RC complex inside FSM particles, which outer sizes are around 1−2 μm, can provide electrons to the dyes in the outer medium or can induce electric current on the ITO electrode with elevated heat stability.

As shown in Table 1 and reported in the literature,[1−3,8−15] many proteins have been incorporated into silica nanopores. Most of them are water-soluble proteins with a small molecular size. These proteins have been shown to retain their functions. Therefore, silica mesoporous materials can be a matrix to fix proteins without severely changing their structure. The structure/activities of these proteins inside silica pores, however, have not been well characterized. The RC protein used in this study is one of the largest protein system that have been incorporated into silica nanopores, and this, together with our previous study on LH2 binding,[15] also indicated that large membrane proteins can fully retain their high functional abilities in silica nanopores. The amounts of the RC and LH2 bound to the FSM were higher than those of the soluble proteins as seen from Table 1. The structural feature of the membrane protein with high hydrophobicity seems to be important for the better adsorption/function into nanopores, although the mechanism is not clear yet.

The pigment−protein complex also has an advantage, namely, to enable the study of the protein behavior inside silica nanopores, because of the multiple prosthetic groups that can be monitored directly. The information deduced from the RC−$FSM_{7.9}$ conjugate will be useful for the use of silica mesoscopic materials as the matrix for new reactions.[1−8] The visible/FTIR difference spectra of the RC induced by the chemical and photochemical reactions were almost the same in solution and in $FSM_{7.9}$. The results indicate that almost all the RC complexes inside nanopores retain their intact structure, except the very minor modifications such as the slight shifts of pigment Qy absorption bands, and can undergo photochemical oxidation/reduction cycle of P885.

The results of the N_2-adsorption isotherm suggest the incorporation of the RC complex into the nanopores of $FSM_{7.9}$. It is shown that LDAO molecules partially decreased the effective pore volume and that the absorption of the RC protein further decreased the volume, suggesting the adsorption into the nanopores. We can also assume another possibility that the RC inhibited the N_2-adsorption just by covering the outer surface of $FSM_{7.9}$. However, this mechanism does not interpret the 15 times larger amounts of RC bound to $FSM_{7.9}$ because $FSM_{7.9}$ and $FSM_{2.7}$ have similar properties of outer surfaces, with similar physicochemical features and particle sizes. It is also clear that $FSM_{2.7}$ could bind RC only to the outer surface, but not to the inner pores. In addition, there is no good reason to deny the adsorption of RC into the 7.9 nm pores inside $FSM_{7.9}$. The pores have a certain range of distribution of sizes and can absorb LDAO molecules well. The increase of the thermal stability also seems to be interpreted more easily if the RC binds to the inner pores. We, therefore, assume that $FSM_{2.7}$ binds the RC mainly at its outer surface and that $FSM_{7.9}$ binds the RC both at the outer surface and inner pores as assumed previously for LH2.[15] The idea also interprets the higher amounts of bindings to $FSM_{7.9}$ and $FSM_{9.0}$ compared to that to $FSM_{2.7}$ in the presence of Triton X-100 shown in Table 1. Direct detection of the RC in FSM in future will give a firm conclusion for the localization and orientation of RC inside the nanopores.

The ratio of adsorbed RC to $FSM_{2.7}$/$FSM_{7.9}$ was 0.02/0.29 (= 7%) from Table 1. We estimated the amounts of the RC bound to the outer surface and the inner pores of $FSM_{7.9}$ on the basis of the following assumptions that the two types of FSM (2.7 and 7.9) have common features with the average pore lengths of 2 μm and the silica wall thickness of 0.3 nm. The assumptions give estimated total pore volumes per unit weight of $FSM_{2.7}$ as 0.84 $cm^3\ g^{-1}$ and $FSM_{7.9}$ as 1.75 $cm^3\ g^{-1}$. The higher specific affinity of the RC to $FSM_{7.9}$ suggests the binding into the silica nanopores. The result, together with the results of an N_2 adsorption isotherm study in Figure 3, supports the idea that the RC is preferentially absorbed into the inner pores of $FSM_{7.9}$. We can assume the amount of the RC bound to the inner pores of $FSM_{7.9}$ to be the difference between the adsorbed amounts of the RC on $FSM_{7.9}$ and $FSM_{2.7}$. On the basis of the assumed amount of 0.27 g RC/g $FSM_{7.9}$ calculated as the difference between the bindings on $FSM_{7.9}$ and $FSM_{2.7}$ in Table 1, we tentatively estimated the average distance between the RCs to be 19 nm inside $FSM_{7.9}$ by assuming the RC to be oriented as shown in Figure 1C. We assume that the interaction between the silica surface inside nanopores and the hydrophobic side surface of the RC, which had been buried within the carbohydrate tails of lipids in the natural membranes and was covered by LDAO molecules after the extraction, might favor the adsorption into silica nanopores. Detergent molecules might fill the small gaps between the RCs and nanopores.

Structure of the RC Inside $FSM_{7.9}$ Studied by ATR-FTIR. The overall protein structure of the RC was essentially unchanged before and after the incorporation into the $FSM_{7.9}$, as confirmed by ATR-FTIR. The IR spectral features of the RC in a free form and in $FSM_{7.9}$ were essentially the same (Figure 4, upper panel). The spectrum of the RC−$FSM_{7.9}$ conjugate retained the amide I band at 1655 cm^{-1}, which is characteristic of the α-helical structure. This indicates that the interaction between the silica surface and the RC protein did not induce severe structural changes in the membrane-spanning domains that are rich in the α-helices in the RC.

The evanescent IR beam from the prism surface penetrates the materials with a typical depth of a few micrometers in the ATR method[33] so that the measured IR spectra of RC−$FSM_{7.9}$ conjugates, with particle sizes of 2−5 μm and silica wall thickness of 0.3 nm, could contain contributions of RCs both on the surface and inside $FSM_{7.9}$. On the other hand, we estimated the surface amount of RC on $FSM_{7.9}$ to be rather low judging from the low amounts of RC bound to $FSM_{2.7}$. Therefore, the IR features in Figure 4 most likely represented the contribution from the RC inside $FSM_{7.9}$. It is also noted that FSM will be useful as capsules to selectively fix large amount of proteins or organic molecules on the prism surface without denaturation.

The "oxidized *minus* reduced" difference IR spectrum of RC−$FSM_{7.9}$ induced by the ferricyanide/ferrocyanide perfusion showed spectral features that were essentially the same as those measured in the RC in the free form. The spectra could represent structural changes upon the changes of the redox state of P885 and the high potential cytochrome *c* heme(s). The IR bands at 1745(+)/1739(−) and 1712(+)/1693(−) cm^{-1} can be assigned to the C_{10}═O ester and the C_9═O keto of the BChl *a* molecules of P885, respectively, by analogy with the redox IR features of other

preparations of bacterial RCs.[32,34] The atomic structure of FSM silica was unaffected by the redox changes in the adsorbed RCs because no additional changes were observed in the Si−O stretch region at 1050−1100 cm^{-1} (Figure 4). The results indicate that the molecular interactions between P885 or heme(s) *c* and functional groups of amino acid residues were almost unaffected after adsorption of RCs into silica pores. Severe structural changes in the peptide chains or direct interaction of redox cofactors in RCs with FSM silica are, therefore, unlikely. Nevertheless, it is likely that the RC protein is somehow in contact with silica walls directly or indirectly judging from the observed 3 nm red shift and 5 nm blue shifts of absorption peaks of BPhe *a* and P885, respectively, and from the increased thermal stability of the RC in $FSM_{7.9}$. The movement of RC protein subunits might be restricted somehow by the nonspecific interaction between the silica walls and the RC protein surface, and the interaction may decrease the chance of irreversible denaturation by the heat treatment.

Reaction Inside Nanopores. Almost all the RC adsorbed to silica nanopores reacted with reagents added to the outer medium. Light illumination also induced the photo-oxidation of the special pair P885 as monitored by absorption changes. The electrons on P885 were transferred to BPhe *a* and then to the artificial electron acceptors VK_3 and to DCIP added into the outer medium. The ability was fully retained in all the RC complexes bound to $FSM_{7.9}$ that gave almost the same extents of absorption changes as that in the RC in solution if normalized by the RC content. The RCs and RC−$FSM_{7.9}$ conjugates pasted onto the ITO electrodes induced photocurrent by the illumination at 890 nm. The activity continued for more than a day at room temperature. The photocurrent detected with the RC−$FSM_{7.9}$ conjugate was a little lower than that with the RC in solution under the present conditions. The current, however, might be increased if the adsorption technique of RC−FSM conjugate to the electrode surface is improved together with the optimization of the mediator system.

Incorporation of the photosynthetic RC into the mesoscopic porous silica thus has opened new chances for the stabilization/fabrication of photosynthetic RC as well as LH2. The silica nanoporous materials provide a reaction environment suitable for the membrane proteins, such as that inside liposomes. Reactant molecules as well as the medium molecules will have restricted motions inside the silica nanoporous materials. The concentration changes of reactants might become higher transiently inside the pores than those in the outer space depending on the feature of diffusion process. The FTIR measurement indicates that RCs have structures that are essentially the same as those inside an aqueous outer medium and undergo similar structural changes of RC protein upon the oxidation of P885. This agrees with the observation that the redox reagents added to the outer medium reduced/oxidized P885 rapidly.

Mechanism of the Stabilization of the RC Inside FSM Nanopores. FSM is known to adsorb many proteins and, in some cases, has been claimed to stabilize the protein structures, as shown in horseradish peroxidase,[8,9] amylase,[13] lipase,[14] and hemoglobin.[12] The stabilization mechanisms, however, have not been clarified. We previously showed that the LH2 became heat-stable in $FSM_{7.9}$ as a first example of the membrane protein incorporated into the silica nanopores.[15] The result with the RC protein in this study indicated that the high adsorption to the FSM and the increase of the heat resistance are the common features of membrane proteins. However, the results of FTIR and optical measurements suggest the interaction between the RC and $FSM_{7.9}$ to be rather weak and induces only shifts of absorption bands of pigments. LH2 showed slightly larger shifts of absorption bands and fluorescence bands of the BChl *a* exciton bands.[15] It is, therefore, assumed that the large motion of the protein subunits that leads to the destruction at the elevated temperature may be restricted inside silica nanopores. Our preliminary result with LH2 suggests that adsorption to the FSM suppresses the irreversible change of the protein structure.

The incorporation of the RC protein into the mesoscopic porous silica brought the stabilization/fabrication of the RC. The RC behaves as it does inside water although free movement from silica pores into the outer medium was restricted. The use of nontoxic silica nanoporous materials as the matrix for the function of the photosynthetic RC protein produced a new photoreaction system without membranes. The membrane proteins can be safely stored inside silica pores, retained higher structural stability, and still react with a reagent outside the membranes. Short-term dehydrations did not inactivate the RC−FSM conjugate. Proper matching of the pore size, material structure, and proteins will contribute to the production of new functional systems with high efficiency and torelancy. We will be able to prepare conjugates of silica mesoscopic materials with multiple enzymes, such as hydrogenases, which can utilize the reducing power from the RC for the production of useful materials.

Acknowledgment. We are grateful to Tsunenori Nozawa and Masayuki Kobayashi (Tohoku University) for providing us *Tch. tepidum* and for their very kind advices on the culturing and the preparation of the RC complex. We also thank Drs. Peter R. Rich and Santiago Garcia for the development of ATR-FTIR equipment (UCL). The work was supported by a Grant-in-Aid from MEXT Japan (No. 19370064) to S.I.